7th Annual International IEEE EMBS Conference on Neural Engineering
Montpellier, France, 22 - 24 April, 2015

Semi-chronic chamber system for simultaneous subdural electrocorticography, local field potentials, and spike recordings

Amy L. Orsborn, Charles Wang, Ken Chiang, Michel M. Maharbiz, Jonathan Viventi, and Bijan Pesaran

Abstract— **The brain operates on many different scales, from individual neurons to interacting cortical areas. Similarly, electrophysiology can monitor neural activity at a variety of spatial resolutions. Yet the majority of electrophysiology studies focus on a single scale of measurements. Simultaneously monitoring neural activity at multiple spatial scales will be critical for better understanding neural processing and developing neuroprosthetic applications. Here, we address the technical challenge of integrating multiple recording modalities into a chronic recording system. We developed a semi-chronic chamber-based system for non-human primates to simultaneously record subdural micro-electrocorticography (μECoG), local field potentials (LFPs) and action potentials in the same tissue volume. The system combines subdural μECoG array recordings with a microdrive and uses a chamber system and artificial duras to align each component. We present the system design and validation of subdural μECoG recordings using artificial duras. Acute recordings from one non-human primate subject are shown to validate the technique.**

I. Introduction

Complex behaviors like dexterous movements and decision making are governed by a host of brain areas. Taking a sip of coffee involves interactions of millions of neurons spread across different brain areas, from visual areas to locate the cup to motor cortices to implement the movement. What scale of neural activity—the individual neurons, or larger networks of neurons—is most relevant for understanding and restoring neural function?

Electrophysiology techniques can be used to measure neural activity at many different spatial scales. Penetrating electrodes inserted into the cortex can record action potentials ("spikes") of individual neurons. Lower-frequency electrical fields immediately surrounding these electrodes (local field potentials, LFP) are thought to reflect summed synaptic activity of neurons within 250 μm around the electrode [1]. Electrodes on the cortical surface (electrocorticography, or ECoG) capture activity of potentially larger and more superficial neural populations. Spiking, LFPs, and ECoG may reflect different aspects of neural function, and the relationship between these measurements is still an area of active research [2]. These signals and recording methodologies also have distinct properties which may influence their utility for neuroprosthetic devices [3].

The majority of electrophysiology studies to date focus on a single scale of neural activity. This is due in part to technical challenges inherent in integrating multiple recording techniques. Few platforms exist to chronically monitor neural activity across multiple spatial scales in awake, behaving subjects. Such platforms will be critical for understanding relationships between individual neurons and larger-scale brain networks, and their relationship to behavior. They will also play an important role in developing neuroprosthetic devices to restore neurological function.

In this paper, we present a platform to simultaneously measure electrophysiological signals at multiple scales within the same volume of cortical tissue. We develop a semi-chronic chamber system that integrates subdural μECoG recordings and a multi-electrode microdrive for non-human primates. We describe the system design and methodological details, and present preliminary recordings from a non-human primate to demonstrate system viability.

II. System Design

A. Overview

We developed a semi-chronic system for simultaneous recording of μECoG, LFP, and spikes in the same volume of tissue (Fig. 1). The system combines recordings with a custom subdural μECoG array with a commercially-available semi-chronic 32-channel microdrive system (Gray Matter Research) [4]. μECoG arrays are custom-designed with holes to allow penetrating electrodes of the microdrive to record LFP and spiking activity form the tissue directly beneath the μECoG array. The microdrive has independently movable electrodes to record in depth across cortical layers.

We use a chamber to house the drive and recording hardware. In the current design, the chamber is 2.6cm in diameter, specified to fit the 32-channel microdrive. Due to the large diameter, chambers are custom shaped to the subject's skull based on magnetic resonance images (using Brainsight, Rogue Research). Chambers are made of PEEK plastic to maintain imaging compatibility and manufactured by Gray Matter Research. The system is affixed to the skull via MetaBond (Parknell Inc.) and dental acrylic.

The chamber also allows us to precisely align the μECoG array and microdrive to within 250 μm. The μECoG array is embedded within an "artificial dura" (AD; see section II.B). ADs have been successfully used for chronic optical imaging in primates [5-7]. We use this approach to ensure the health of neural tissue upon removal of the dura and to precisely

*Research supported by a New York University Grand Challenge Grant (BP and JV) and the Defense Advanced Research Projects Agency contract W911NF-14-2-0043 (BP).

A.L. Orsborn and B. Pesaran are with the Center for Neural Science, New York University, New York, NY 10003 USA.

C. Wang, K. Chiang, and J. Viventi are with the Department of Biomedical Engineering, Duke University, Durham, NC 27708, USA.

M. M. Maharbiz is with the Department of Electrical Engineering and Computer Science, University of California, Berkeley, CA 94720 USA.

Corresponding author: Bijan Pesaran (email: bijan@ nyu.edu)

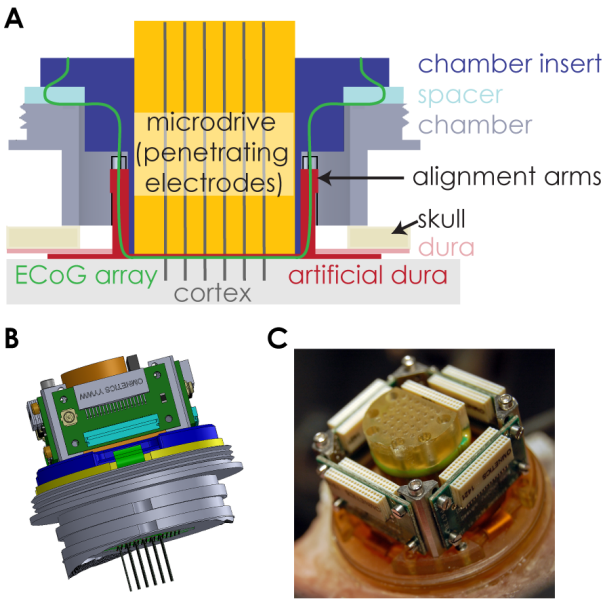

Figure 1. Chamber system design. (A) Schematic showing a cross-section view of the chamber. Note that data acquisition hardware is not shown. (B) Computer design drawing of the full system, including data acquisition PCBs. (C) photograph of an implanted chamber system.

place the ECoG array within the chamber. The custom artificial dura has spokes that mate with groves in the chamber to fix the array location (Fig. 1a; Fig. 2a-d).

The chamber is sealed using a custom insert that mates with the artificial dura (Fig. 1a). Rubber spacers are used to adjust the total height of the system, allowing tolerance in estimating the height of the cortical surface relative to the skull. The microdrive sits inside the chamber insert.

Finally, ports for data acquisition are housed on top of the chamber (Fig. 1b, c). Data from the µECoG array and microdrive are routed to 34-pin Omnetics connectors via custom printed circuit boards. The current design allows access to 256 channels of ECoG data and the 32 microdrive electrodes. The chamber and hardware are sealed with a chamber cap, maintaining sterility for chronic recordings.

Our design has several notable features. ADs can be removed and replaced. This is useful in the event of hardware failures, and could also be used to study how ECoG array parameters (e.g. contact size, materials) impact recording quality. The microdrive system allows measurement from the full cortical volume beneath the µECoG array. Finally, the design is highly modular. It can be used for chronic µECoG or microdrive recordings alone. Data acquisition hardware can be changed to increase channel counts. Electrical and optical stimulation hardware could also be integrated. The design is also scalable for recording larger cortical volumes.

B. Artificial dura and ECoG electrode array molding

Our approach uses an artificial dura (AD) to protect the brain while acquiring access for subdural ECoG recording [5-7]. The AD is made of silicone (Momentive RTV615). We designed and fabricated custom aluminum mold pieces to form an AD shaped to mate with our chamber (fig. 1a; fig. 2).

The silicone AD has several desirable properties. First, it is optically clear, as seen in Fig. 2a. Optical clarity of manufactured ADs was tested using a photodiode to measure laser intensity changes after passage through the AD. Our tests indicate that the AD allows 75%-80% passage of 473 nm light. Clear ADs allow our technology to be integrated into optogenetic approaches [e.g. 7], and aid in visualizing neural and vascular structures underneath the µECoG array once implanted (Fig. 2d). The silicone also cures at room temperature, allowing us to cure ECoG arrays within the silicone without application of heat. Finally, the silicone is highly flexible, and conforms to the brain surface.

µECoG arrays are embedded within the AD. The array is encapsulated within the silicone while exposing the contacts on the bottom of the array (Fig. 1a; Fig. 2b-d). The embedding process includes initial placement and sealing the array edges, followed by molding the full AD. Alignment of the µECoG array within the AD is critical for assuring alignment of the array and microdrive. A custom-designed holder guides placement of the array onto the base of the AD mold and pin the µECoG array to mold. Silicone is applied to the edges of the array and allowed to cure, adhering the array to the mold surface in precise position. The custom holder is then removed, and the full mold is assembled around the ECoG array. Silicone is poured into the mold and cured to create the final AD with embedded array (Fig. 2b-d). Kapton tape is used to protect electrode contacts during the molding process and removed just prior to implantation.

III. Methods for System Validation

A. Array molding validation

To test the viability of the embedding procedure, the impedance of array contacts was tested after embedding within the AD. Impedances were measured with a NanoZ multi-electrode impedance meter (Neuralynx) at 1004 Hz. Three ECoG arrays were measured; two of which were tested both before and after molding to test for significant changes.

B. Acute electrophysiology recordings

The full chamber system was implanted and used for recordings in an acute preparation from one non-human primate (*macaca fascicularis*). The subject was anesthetized and paralyzed (Sufentanil and Atracurium) during surgical procedures and recordings. The chamber was implanted over the post-central gyrus, approximately primary somatosensory cortex (S1). All procedures were conducted in compliance with the National Institute of Health Guide for Care and Use of Laboratory Animals and were approved by the New York University Institutional Animal Care and Use Committee.

A craniotomy and durotomy were performed. An AD with an embedded µECoG array was implanted within the durotomy (Fig. 2d). The custom array had 124 contacts, 200 µm in diameter and 0.75 – 1.5 mm spacing (non-uniform; see Fig. 2e for geometry of contacts). The array was composed of polyimide with 5 µm thick Copper, 3 µm Nickel, and 150 µm Gold traces and contacts. Copper and nickel interlayers are not biocompatible but the tissue is protected from these by a surface layer of gold. This technique has proven successful for chronic use [8]. The array included 32 500 µm diameter holes for the microdrive electrodes. Contact leads were routed to four ZIF connectors which attached to chamber-mounted PCB boards for data acquisition.

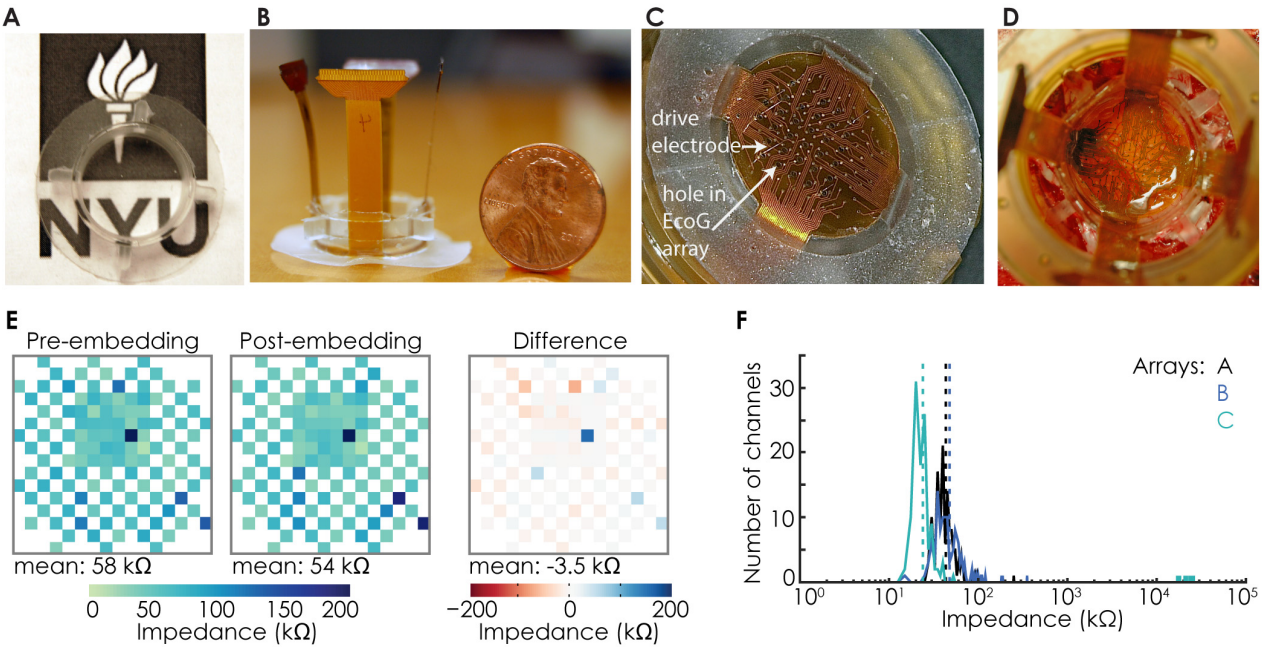

Figure 2. Embedding ECoG arrays into artificial duras (ADs). (A) A silicone AD shaped to mate with our chamber system, sitting on the NYU logo to demonstrate clarity. (B) Side-view of a µECoG array embedded within an AD. (C) Bench test of alignment between µECoG array and microdrive electrodes. Drive electrodes penetrated the holes of the µECoG array. (D) Embedded array implanted over the post-central gyrus. (E) Impedance of an example array before and after embedding (left, middle) and the change in impedance (right). White portions note the absence of a contact. Contact distribution across the array was non-uniform, with increased density in a middle portion overlapping with the microdrive. (F) Histogram of measured impedances across channels for 3 tested arrays post-embedding. Dashed lines show median impedance across each array.

A 32-channel microdrive was then installed. The drive was loaded with 250 µm diameter glass-coated Tungsten electrodes (Alpha Omega); average impedance of 1.4 MΩ, range: 0.4 – 3.5 MΩ (measured at 1 kHz). Drive electrodes were spaced 1.5 mm apart and attached to shuttles which allow them to be independently moved. See [4] for details.

Data was acquired using a 128-channel Cerebus system (Blackrock Microsystems). Broadband data were simultaneously collected at 30 kHz from the microdrive (32 channels) and 96 channels of ECoG contacts. In post-processing, data were band-pass filtered into local field potentials (0 – 300 Hz) and multi-unit activity (> 300 Hz). LFPs were downsampled to 1 kHz. Spikes were defined via threshold crossings using a threshold of 3.5 standard deviations from the mean filtered multi-unit trace.

Recordings were taken as drive electrodes were lowered through the cortical tissue. Electrodes were initially advanced until the tips were exposed from the drive but not yet in the brain (estimated at time of drive assembly and by visual inspection of recordings). This was defined as 0 depth. Electrodes were then lowered (uniformly across all drive electrodes) in 0.25 – 0.5 mm increments spanning 3.75 mm. Recordings were collected at each depth for 2-3 minutes.

IV. Results

A. Array embedding validation

Figure 2e shows a comparison of contact impedances for an example µECoG array before and after AD embedding. For this array, we found little change in impedance after embedding (-3.47 kΩ average change, $p < 0.05$ paired Wilcoxon sign-rank test; 6% relative change in average impedance across the array). Across three embedded arrays, the contacts were typically low impedance (Fig. 2f; Median impedance post-embedding: A = 42 kΩ; B = 45 kΩ; C = 24 kΩ). However, embedding yielded high-impedance contacts in one instance (array C), likely caused by silicone encapsulation. This only impacted a small fraction of contacts (13 of 124, or 10%). Together, this demonstrates the viability of embedding ECoG arrays in an AD for recordings.

We also performed a bench test to validate alignment of the µECoG array with the microdrive. The chamber system was assembled with an embedded µECoG array. Microdrive electrodes were then lowered until they penetrated the AD. Visual inspection with a microscope showed that all electrodes (250 µm diameter) passed through the holes (500 µm diameter) in the µECoG array (Fig. 2c), confirming alignment of our system within 250 µm of precision.

B. Acute neural recordings

Figure 3 summarizes the neural recordings obtained from our system in the acute recording test. Raw data for an example microelectrode and µECoG array (Fig. 3a) across recording depths shows a clear progression through the cortex. Multi-unit and LFP traces from the drive are flat at superficial depths prior to entering the cortex. Signal amplitudes increased and spiking activity was found as the electrode moved through the cortex. The µECoG signal for each depth recording, however, remains at relatively constant amplitude. Figure 3b quantifies the changes in signal amplitude (RMS for LFP and µECoG; mean spiking rate for multi-unit activity) as a function of depth across the recorded electrodes. µECoG amplitudes remained stable across the recordings (as anticipated since only drive electrodes are moving). LFP amplitude, however markedly increases starting around 1.75 mm. The LFP amplitude change is

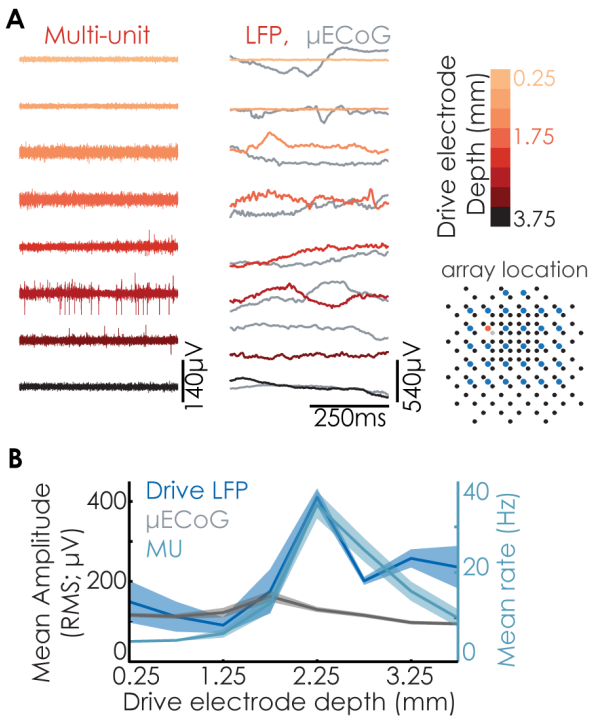

Figure 3. Data from acute recordings. (A) Raw data (multi-unit, right; LFP and µECoG, left) for an example drive electrode and nearby µECoG contact for recordings at different drive electrode depths. Color indicates recording depth (MU and LFP; µECoG shown in grey because depth does not change). Schematic illustrates the location of the example drive electrode and µECoG contact. (B) Signal amplitude (RMS) and MU firing rate as a function of drive electrode depth. Solid line shows the average across all drive or µECoG electrodes; shading denotes SEM.

paralleled by firing rates across the array. These recordings demonstrate the feasibility and viability of our recording system. Though beyond the scope of this abstract, these data can also be used to probe relationships between LFP and µECoG signals across depth and the cortical surface.

We found multi-unit activity on the majority of the drive (30 of 32 electrodes). Viable multi-unit activity was determined by spike rates exceeding a baseline threshold. Baseline was defined as 4 standard deviations from the mean spike rate on the drive at 0 depth (i.e. before entering the brain). Microdrive channels showed significant multi-unit activity at 3.4 ± 1.3 depths (mean ± STD). Visual inspection of the explanted µECoG array also showed no signs of damage, further corroborating that microdrive electrodes successfully passed through the holes into the brain.

V. Discussion and Conclusions

We present the design and validation of a semi-chronic chamber system for multi-scale neural recordings in non-human primates. Our design uses artificial dura techniques [5-7] to solve the challenge of aligning a µECoG array and microdrive for simultaneous recordings. Our bench test and acute recordings demonstrate successful alignment within 250 µm tolerance. We also present data showing the feasibility of embedding µECoG arrays into ADs. Together this report shows the feasibility and viability of our method.

The presented data—simultaneous µECoG and microdrive data across many depths—show the promise of multi-scale recordings. This data can be used to investigate relationships between neural signals, such as the relative amplitude of ECoG vs. LFP (Fig. 3). Our results also suggest that relationships between ECoG and LFP could be used to triangulate the depth of microdrive electrodes to better facilitate studies of information across cortical layers [4].

The chamber system is designed to facilitate chronic recordings. Additional longitudinal testing is needed to assess the system's long-term viability. ADs have been successfully used for chronic imaging for months to years [5-7]; ADs with embedded ECoG arrays must also be tested.

Our system design is modular, providing a powerful platform for multi-scale recording and manipulations. The chamber can be used for chronic µECoG or microdrive recordings alone, and can be extended to incorporate optical and electrical stimulation. The AD design also provides flexibility to change ECoG hardware. All modifications can be performed in the same implanted chamber.

Our design can also, in principle, be scaled up to record from larger cortical networks. Curvature of the brain presents a technical challenge for increasing size. µECoG arrays, ADs, and microdrive surfaces must be custom shaped to the brain's curvature. Future efforts will focus on solving these issues and integrating optogenetic stimulation to achieve large-scale, multimodal recordings and manipulation of neural circuits during cognition and behavior.

Acknowledgment

We thank Baldwin Goodell and Yan T. Wong for assistance with chamber system design. We also thank Ryan Shewcraft, Michael Rabadi, Shaoyu Qiao, and Kevin Brown for help during experimental recordings.

References

[1] S. Katzner, I. Nauhaus, A. Benucci, V. Bonin, D. L. Ringach, and M. Carandini, "Local origin of field potentials in visual cortex," *Neuron* vol. 61(1), pp. 35 – 41, 2009.

[2] G. Buzsaki, C. A. Anastassiou, and C. Koch, "The origin of extracellular fields and currents—EEG, ECoG, LFP, and spikes," *Nat. Rev. Neurosci.*, vol. 13, pp. 407 – 420, 2012.

[3] D. R. Kipke, W. Shain, G. Buzsaki, E. Fetz, J. M. Henderson, J. F. Hetke, and G. Schalk, "Advanced Neurotechnologies for Chronic Neural Interfaces: New Horizons and Clinical Opportunities," *J. Neurosci.*, vol. 28(46), pp. 11830 – 11838, 2008.

[4] D. Markowitz, Y.T. Wong, C. M. Gray, and B. Pesaran, "Optimizing the decoding of movement goals from local field potentials in macaque cortex," *J. Neurosci.*, vol. 31(50), pp. 18412 – 18422, 2011.

[5] L. M. Chen, B. Heider, G. V. Williams, F. L. Healy, B. M. Ramsden, and A. W. Roe, "A chamber and artificial dura method for long-term optical imaging in the monkey," *J. Neurosci. Methods* vol. 113(1), pp. 41 – 49, 2002.

[6] A. Arieli, A. Grinvald, and H. Slovin, "Dural stubstitute for long-term imaging of cortical activity in behaving monkeys and its clinical applications," *J. Neurosci. Methods* vol. 114(2), pp. 119 – 133, 2002.

[7] O. Ruiz, B. R. Lustig, J. J. Nassi, A. Cetin, J. J. Reynolds, T. D. Albright, E. M. Callaway, G. R. Stoner, and A. W. Roe, "Optogenetics through windows on the brain in the nonhuman primate," *J. Neurophysiol.* vol. 110(6), pp. 1455 – 1467, 2013.

[8] M. Fukushima, R. C. Saunders, M. Mullarkey, A. M. Doyle, M. Mishkin, and N. Fujii, "An electrocorticographic electrode array for simultaneous recording from medial, lateral, and intrasulcal surface of the cortex in macaque monkeys.," J. Neurosci. Methods, vol. 233, pp. 155–65, Aug. 2014.